BEE4530

Effect of Layout and Shape to the Drug Delivery of Intratumoral Implant

Zhengxing Xue, Yalu Cai, Matthieu Fuchs

Introduction

Cancer is a group of diseases involving abnormal cell growth with the potential to invade or spread to other parts of the body. In 2015, about 90.5 million people had cancer. About 14.1 million new cases occur a year.[1] It caused about 8.8 million deaths (15.7% of deaths).Abdominal cancer is a particular type of cancer that occurs when there is an uncontrolled

growth of abnormal cells anywhere in the abdomen. It is one of the most pernicious types of cancer.[2] Since the abdomen consists of many organs, including the stomach, intestines, liver, gallbladder, and pancreas, abdominal cancer is more difficult to detect and treat. [3-5]

Currently the most curative treatment option for abdominal cancers is surgical resection followed by adjuvant chemotherapy or radiation therapy to minimize the risk of recurrence [6]. Many cancers respond well to this treatment strategy, but many patients are not eligible for surgical resection due to a variety of reasons. For example, cancer of the liver is difficult to treat with resection because more than one liver lobe may be involved and the possibility of a coexisting liver condition (e.g., cirrhosis) [7]. Abdominal cancers, such as those of the pancreas and stomach, also have low resection success rates and poor overall patient survival [9].

Treatment of unresectable tumors has been supplemented in recent years by the development of minimally invasive interventions, such as laser, microwave, and radiofrequency (RF) ablation. [10] RF ablation in particular has shown improved efficacy, where approximately 80% of tumors cannot be surgically removed. However, despite its success, RF ablation is restricted by limited effective ablation volume that can be created with a single treatment as well as the risk of tumor recurrence around the boundary. [11-12]

Biodegradable polymer implants, termed polymer millirods, have been designed to deliver chemotherapeutic agents to the RF treated region to kill residual tumor cells and prevent tumor recurrence. [8] These implants have been studied systematically in non-ablated and ablated liver tissues, and initial studies using doxorubicin-containing implants to treat tumors have indicated their potential benefit. Currently, the major challenge in effectively treating tumors with polymer millirods has been the limited drug penetration distance into the surrounding tissue. Although several changes to implant design have already been described, how these changes would affect local drug delivery and antitumor efficacy is still not known.

In “Modeling doxorubicin transport to improve intratumoral drug delivery to RF ablated tumors”, the researchers built a mathematical model to provide an ideal strategy to optimize intratumoral drug delivery implants to supplement radiofrequency (RF) ablation for tumor treatment [8].They focused on the drug diffusion process in both a one-dimensional (1-D) simulation model and a more complex three-dimensional (3-D) simulation model. According to their experiment data and modeling analysis, they estimated the diffusion coefficient and drug elimination rate in ablated and non-ablated tumors. They found that RF ablation facilitates intratumoral drug delivery in tissue by reducing normal elimination processes and increasing diffusion. Also, they suggested that computational modeling approach has great advantages to design and rapidly prototype new implant treatment strategies.

In "Polymer implants for intratumoral drug delivery and cancer therapy", Weinberg et al. examined different designs of tumor implants to provide optimal drug release kinetics [7]. They examined the delivery goals for the implants and the methods to modulate local drug pharmacokinetics. They used three-dimensional (3-D) modeling to study the effect of using one central implant versus four peripheral implants on the drug diffusion process inside the tumor. The different layouts of the implants can maximize drug coverage of the tumor periphery, but also need to maintain a reasonable number of implants and total drug dose, which needs further exploration.

These two papers discussed above provide us specific parameters for the modeling process and many great ideas for our study. Based on these studies, we are going to create a more realistic model that replicates ablating a tumor in the liver and then delivering a chemotherapy drug, Doxorubicin, intratumorally. While previous research focused on the simplified spherical geometry, we constructed a more realistic three-dimensional (3-D) tumor simulation from a CT scan of the actual tumor. This will provide us with more accurate insight in our exploration of the optimal implant drug delivery.

Problem Statement

In our modeling, assisted by our realistic 3D model, we study the effect of different types of implants and the impact of their drug release profiles on the drug concentration in the tumor, in detail. Inspired by 'one central implant versus four peripheral implants', we modeled different shapes and layouts of the implants to find the optimal solution for liver tumors.

Design Objectives

The design objective of our project is to explore alternative ways of promoting effective implant drug release. We tested improvements to the simple one-cylinder layout in the following steps or stages to enhance the scope and adaptability of our model:

1) Research for the optimal implant(s) layout.

2) Examine the effect of the shape of the implant by switching to spherical and rectangular geometry.

Method

Schematic

A 3-D model was implemented into COMSOL Multiphysics to model the diffusion from the implant into the tumor. The tumor model is realistic and is obtained from scanning [15] (see Fig. 1).

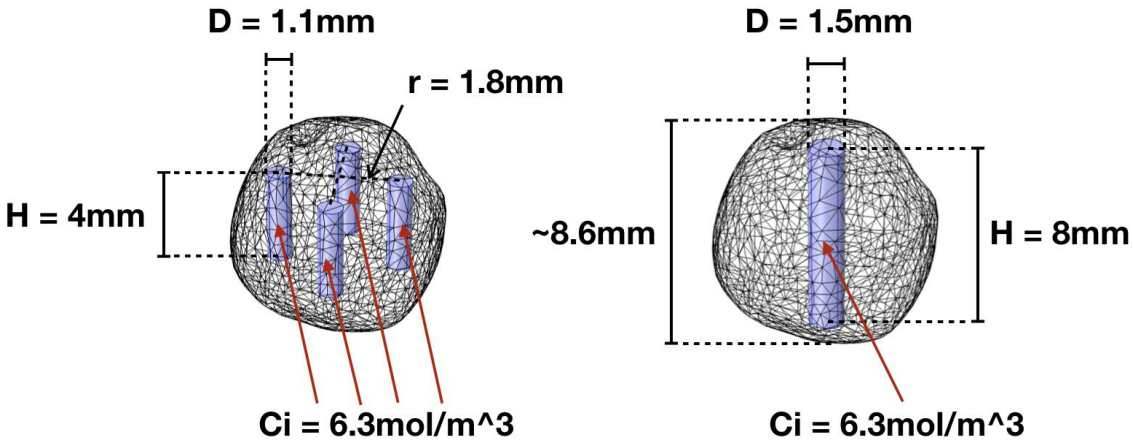

Figure 1: **The two primary layouts that we are modelling**. The right schematic shows a single implant in the center of the tumor and the left schematic shows 4 implants scattered evenly on a circle whose center is the tumor center and radius is 1.8mm.

In Fig. 1, the diffusion direction is from the implant to the tumor, as is depicted in Fig. 2.

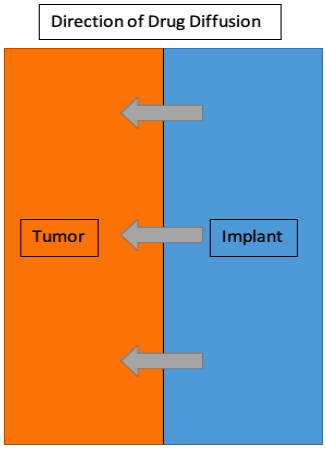

Figure 2: **direction of diffusion**: from implant to the tumor.

The implant is small enough to fit in the tumor, and its specific measurements are shown in Fig. 3.

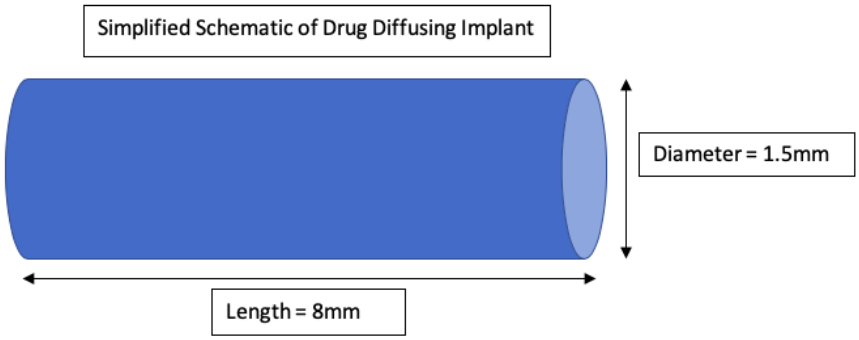

Figure 3: **Dimensions of the implant**, which has a diameter of 1.5mm and a length of 8.0mm.

Governing Equations

The physical process of our model can be described by the 3D transient diffusion equation with first order reaction ($Eq.1$), where C is the concentration of doxorubicin, D is the diffusivity and $\boldsymbol{\gamma}$ is the elimination rate. All the parameters can be found in Table A1 in the appendix.

$$\frac{\partial C}{\partial t} = \nabla(D\nabla C) - \gamma C \qquad Eq.1$$

It is worth mentioning that due to the self-healing process of the tumor, $\boldsymbol{\gamma}$ is 0 from t=0d to t=4d. The exact value can be retrieved in Table A1 in the appendix.

Boundary Conditions

For a single implant, We have two boundary/initial conditions for our model.
First, at time 0, the drug concentration inside the implant ($0 \leq r \leq R_{IB}$) volume is a uniform initial value C_i Second, the outer boundary ($r = R_{OB}$) of the tumor has zero flux. ($Eq.2$).

$$C(inside\ the\ implant, \quad t = 0) = C_i$$

$$q''(boundary\ of\ the\ tumor) = 0 \qquad Eq.2$$

For the 4 implants case, similarly, at time 0, the drug has a uniform value. The outer boundary of the tumor is also fixed at zero concentration. ($Eq.3$)

$$C(inside\ the\ implant, \quad \theta = 0°, \quad t = 0) = \frac{C_i}{4}$$

$$C(inside\ the\ implant, \quad \theta = 90°, \quad t = 0) = \frac{C_i}{4}$$

$$C(inside\ the\ implant, \quad \theta = 180°, \quad t = 0) = \frac{C_i}{4}$$

$$C(inside\ the\ implant, \quad t = 0) = \frac{C_i}{4}$$

$$q''(boundary\ of\ the\ tumor) = 0 \qquad Eq.3$$

All the parameters can be found in Table A1
in the appendix.

Mesh

The following meshes (Fig. 4) are created by COMSOL Multiphysics with *Physics-controlled mesh* method and *Finer* element size.

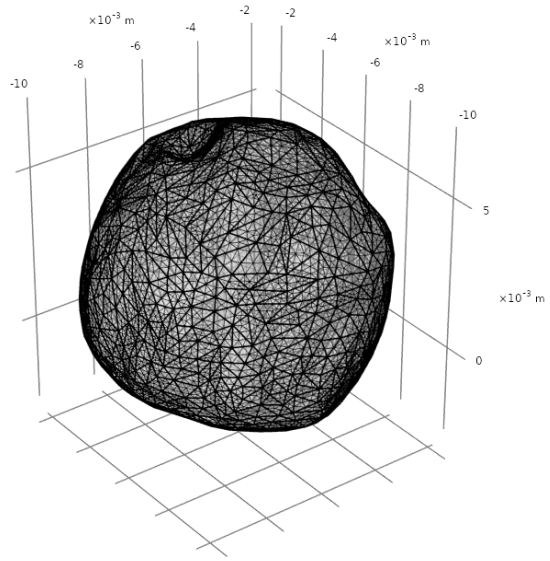

(a)

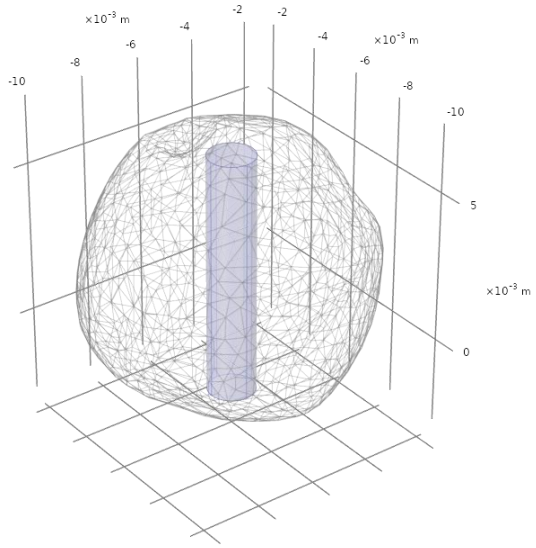

(b)

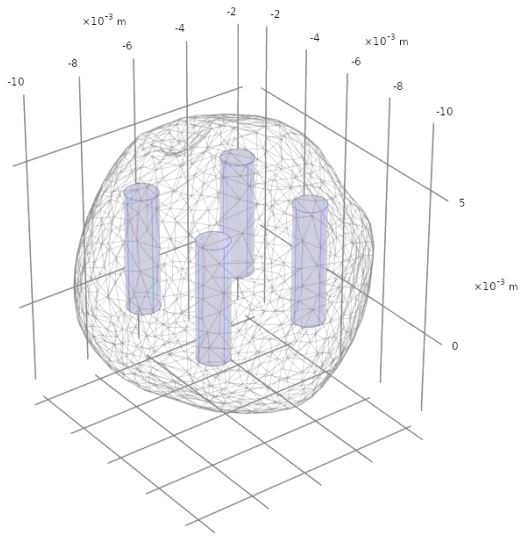

(c)

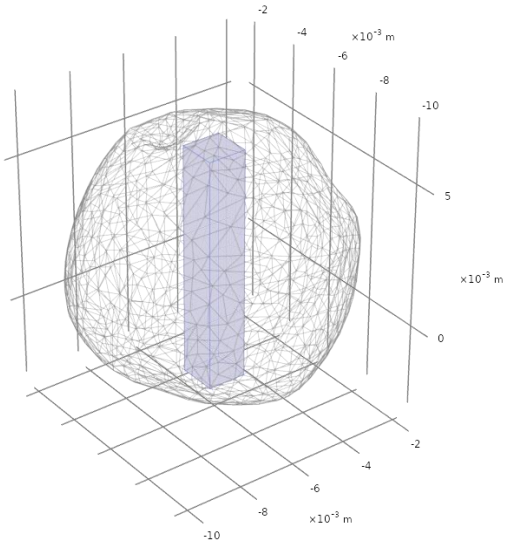

(d)

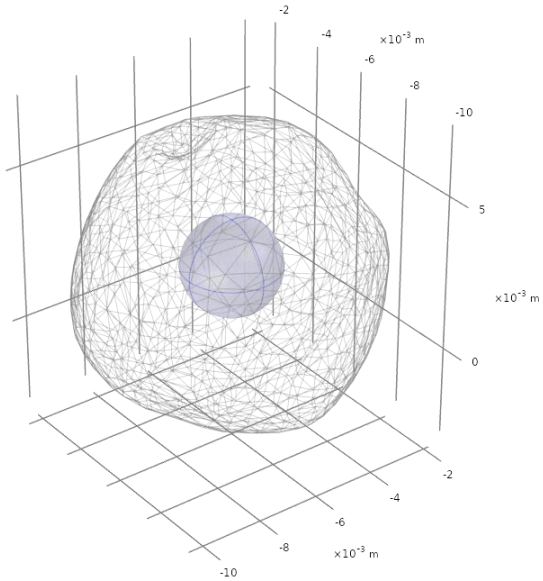

(e)

Figure 4: ***Models showing the tumors analyzed to understand drug diffusion over time****. (a) shows the mesh of the tumor with the implant hiding. (b) shows the model with the mesh that was used to analyze a single implant. (c) shows the 4 implant scenario. (d) shows the rectangular implant scenario and (e) shows the spherical implant scenario.*

Results & Discussion

Mesh Convergence

The analysis was performed using an extremely coarse, extra coarse, coarser, coarse, normal, fine, finer, extra fine and extremely fine mesh. The variable we chose for analysis is the average concentration at t=5d, which can represent both the effect of diffusion and elimination. Fig 5 shows that mesh convergence occurs at approximately 300000 mesh elements.

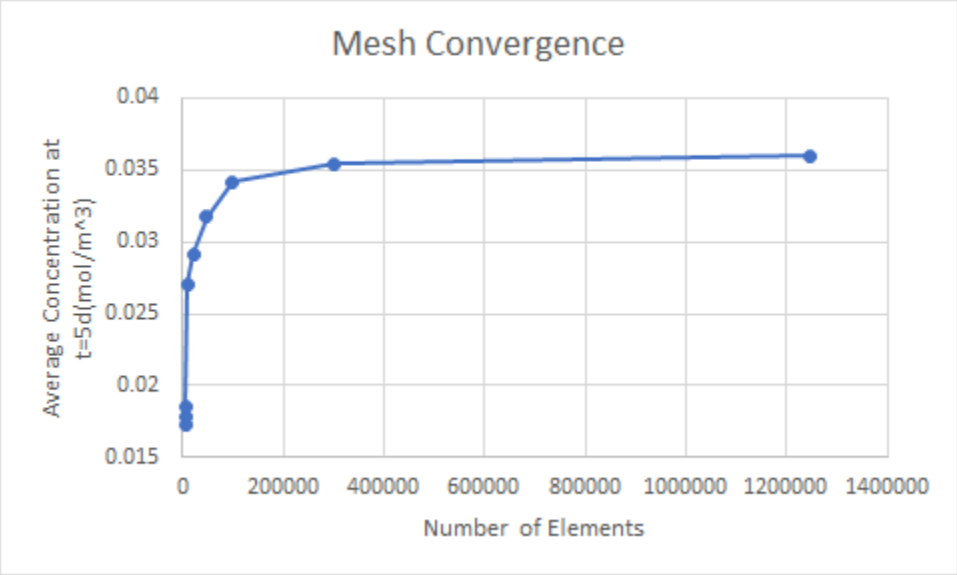

Figure 5: **Mesh convergence analysis plot**. Average concentration at t=5d is plotted against the number of mesh elements.

Concentration Profiles

Since one of our primary goals is to understand the diffusion-elimination process in 8 days after ablation, it is worthwhile for us to obtain the concentration profile at different times in the process.

As the process begins, doxorubicin starts to diffuse out of the implant, into the tumor and eventually is decayed inside the tumor. At first, the process is purely diffusion, since the ablation has deprived the tumor tissues of the ability to carry on normal activities. However, from t=4d, we believe that the tumor will start to heal[8], and will gradually regain its ability to eliminate the drug. Fig. 5, Fig. 6, Fig. 7 and Fig. 8 show the concentration profile inside the tumor with different implant shapes and layouts at 0, 2, 4, and 8 days.

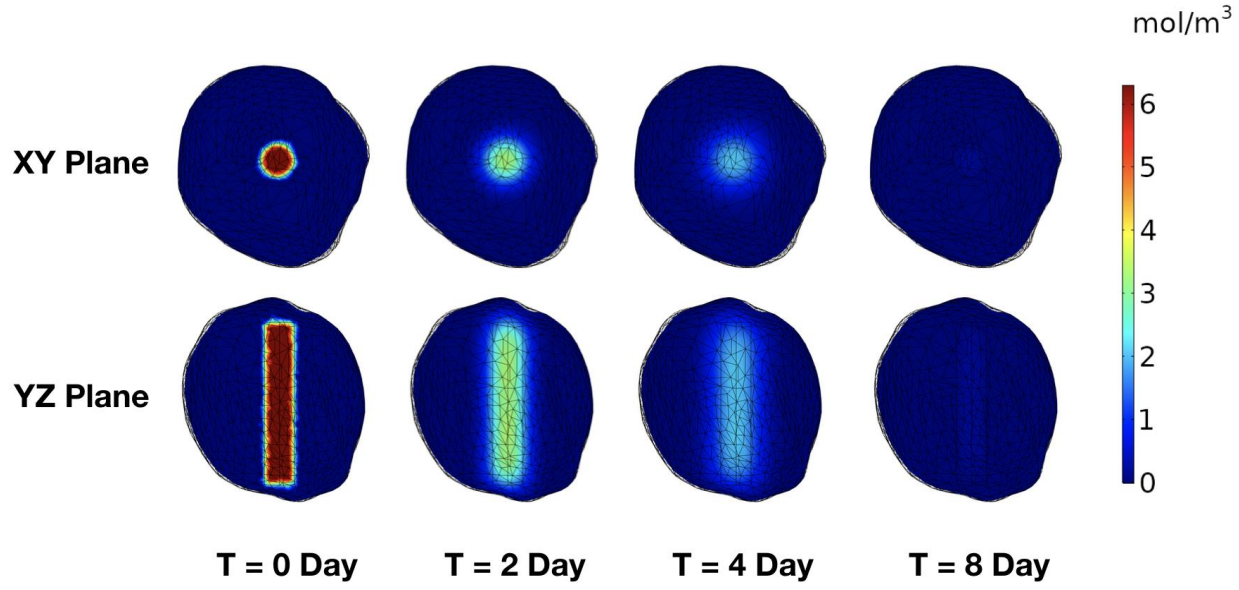

Figure 6: **Concentration profile inside the tumor with a single implant at 0, 2, 4, and 8 days**. At the initial state (t=0 days), there is no drug in the tumor domain and all the drug is inside the implant. When t = 4 days, ~68% drug diffuses out from the implant into the tumor as seen by the reduced 'redness' and increased 'blueness' from the model which correlates to reduced drug concentration inside the implant and increased drug concentration inside the tumor. At t = 8 days due to the drug elimination, there is less drug concentration throughout the implant compared to t = 4 days.

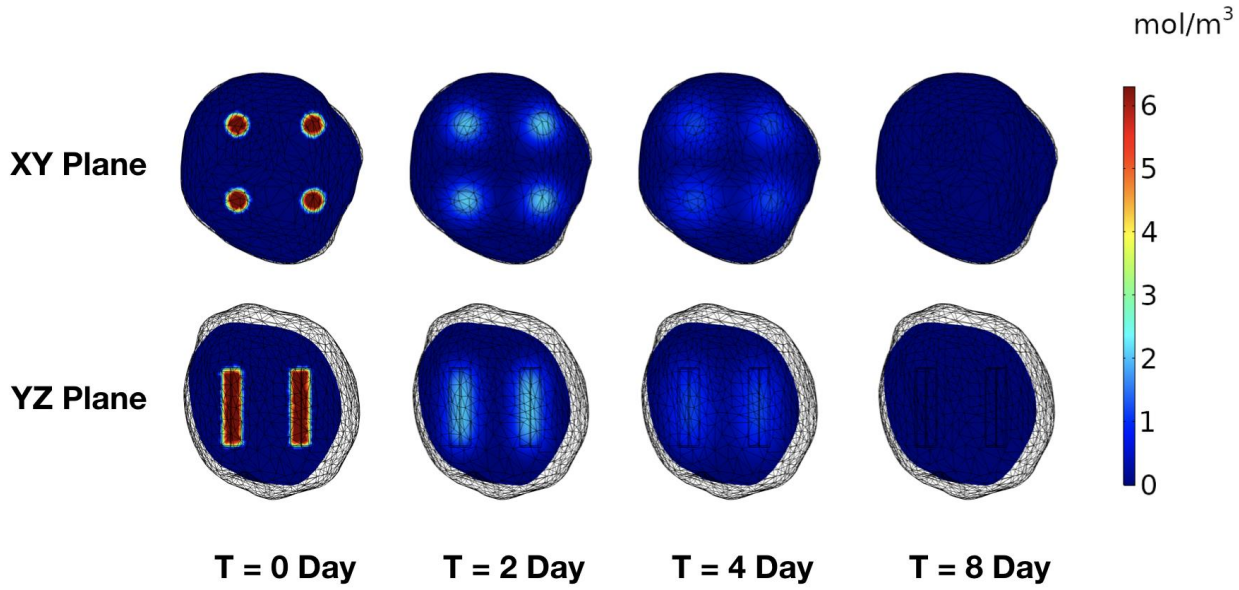

Figure 7: **Concentration profile inside the tumor with 4 implants at 0, 2, 4, and 8 days**. The diffusion process is similar to the tumor with single implants. As there are more contact surfaces, the drug diffuses out the implants more quickly. When t = 2 days, ~68% of the drug has diffused out from implants to the tumor. When t = 4 days, ~83% of the drug has diffused out from the implants and starts the process of elimination inside the tumor.

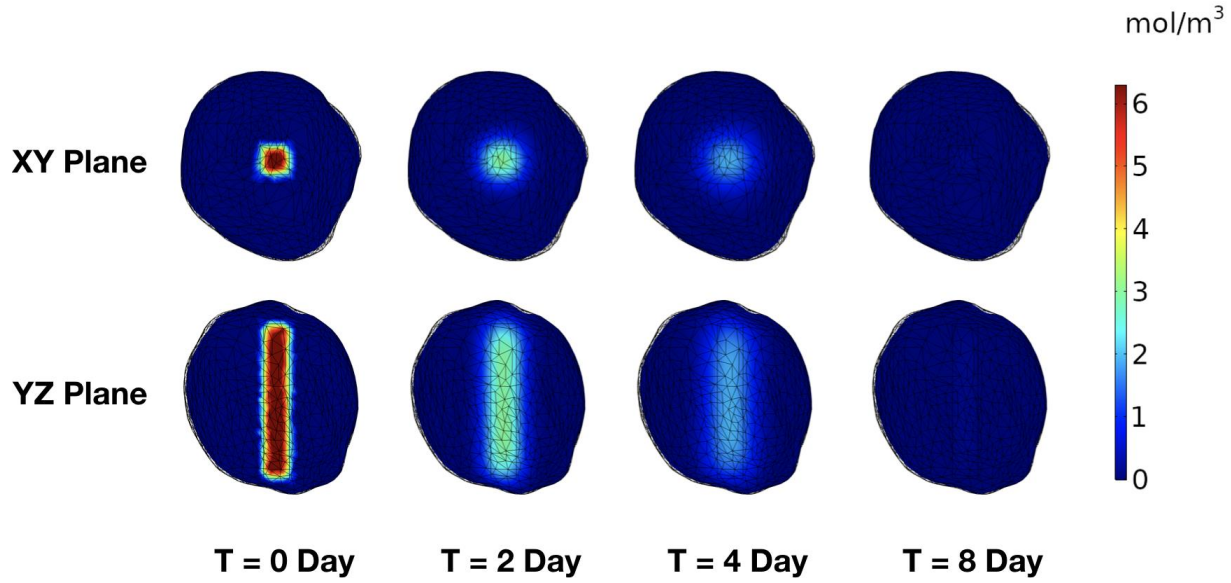

Figure 8: **Concentration profile inside the tumor with one rectangular prism implant at 0, 2, 4, and 8 days**. The diffusion process is similar to the tumor with single implants. When t = 4 days, ~68% of the drug has diffused out from the implants and starts the process of elimination inside the tumor.

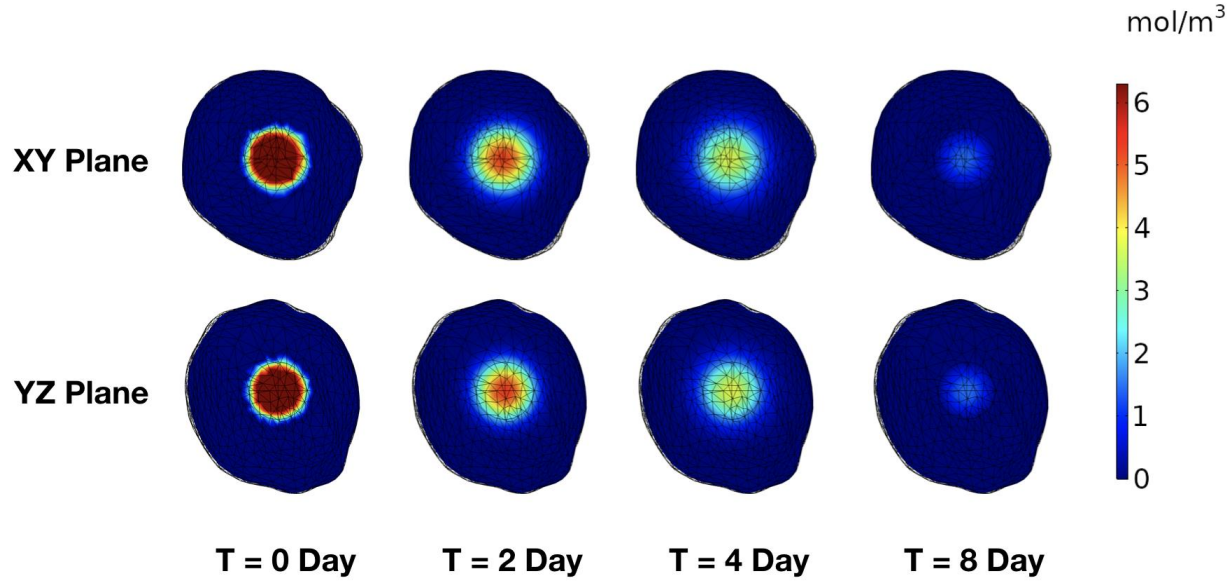

Figure 9: **Concentration profile inside the tumor with one sphere implant at 0, 2, 4, and 8 days**. As the sphere has the least contact area with the tumor, the diffusion process is the slowest. When t = 4 days, only ~50% of the drug has diffused out from the implants and starts the process of elimination inside the tumor.

Average Concentration

Average concentration (Fig. 10) offers a more quantitative view of the effect of our drug diffusion. This is a good measure of how good an implant method is, because high average value means more drugs are in effect inside the tumor. The Four cylinder implants achieve highest average drug concentration in the tumor domain.

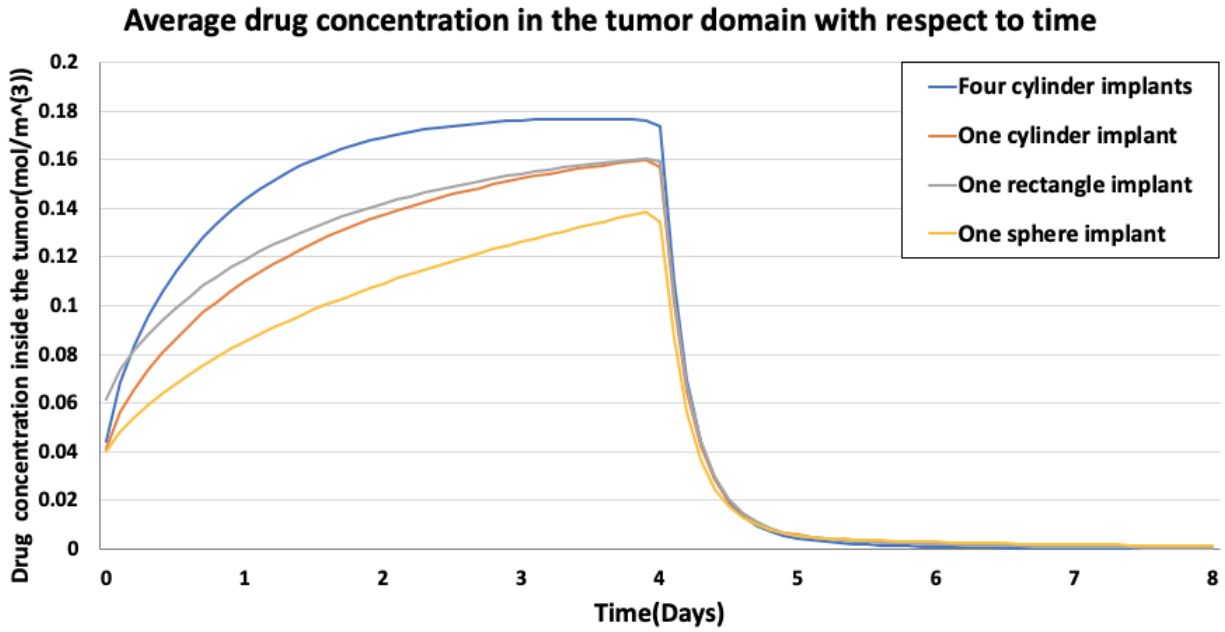

Figure 10: **Average drug concentration inside the tumor with respect to time**, which occured due to diffusion

Notice that the average concentration dropped dramatically after 4d, this is because after 4d, the elimination reaction started. Drug elimination only started after 4d because in clinical trials the ablation completely stopped drug elimination during that time period. However due to reperfusion of the ablated tumor areas, elimination returned to values similar to that in normal tumors between day 4 and day 8.

Validation

We compared our computational results with the experiment results found in Weinberg et al. [8] (Fig. 11).
The variable we are comparing is the concentration of doxorubicin at a different distance from the center. This variable is chosen simply because this is the one measured in the experiment.

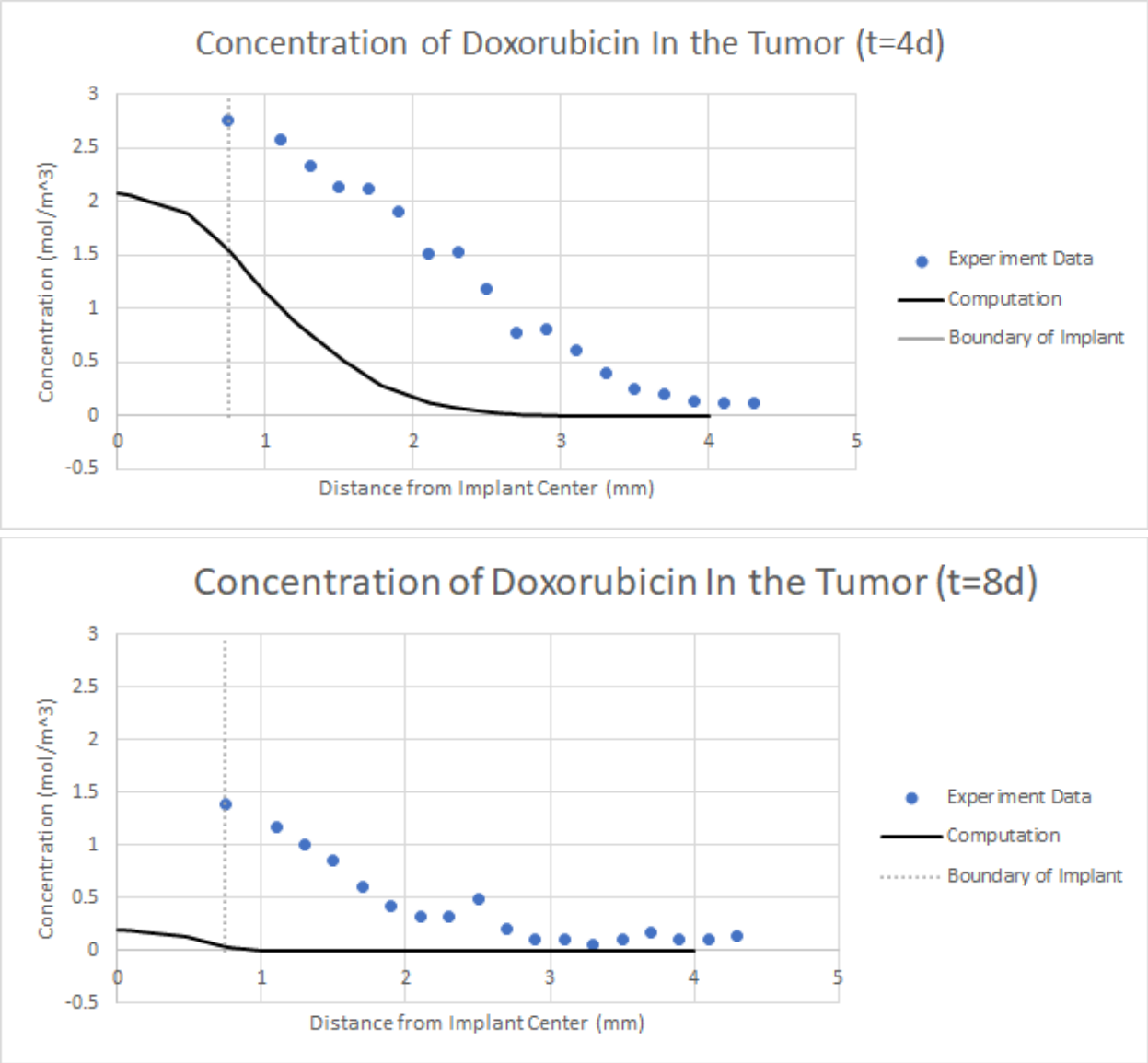

Figure 11: Our model is compared to the experiment result of Weinberg et. al.

From the above comparison, we can observe that the scale and trend of our computational results are comparable to the results of the Weinberg et al experiment, although considerable differences do exist. In this validation, difference is expected since the tumor geometry model that we used isn't the one tested in the experiment. We believe this is because in reality, the doxorubicin elimination rate in the tumor gradually increases from 0 as the tissues heal itself several days after ablation. We were not able to get the elimination rate as a function of time exactly, but had to approach the real function by interpolating the elimination rate value measured at t=8d, while setting t=4d to be the point at which the tissue starts healing.
This approximation is by all means crude, however, it led to the result that modelling at later times is more erroneous.

Sensitivity Analysis

We performed sensitivity analysis by varying five different parameters and computing how these changes affect average drug concentration inside the tumor at day 6. More specifically, we varied initial drug concentration inside implants, drug diffusivity inside tumors, and drug elimination inside tumors, as well as the implant location by 10%. We choose the 10% range, as the biological variability in the material properties of the tumor, due to age, gender, physical activity levels as well as other factors, are assumed to not exceed 10%.

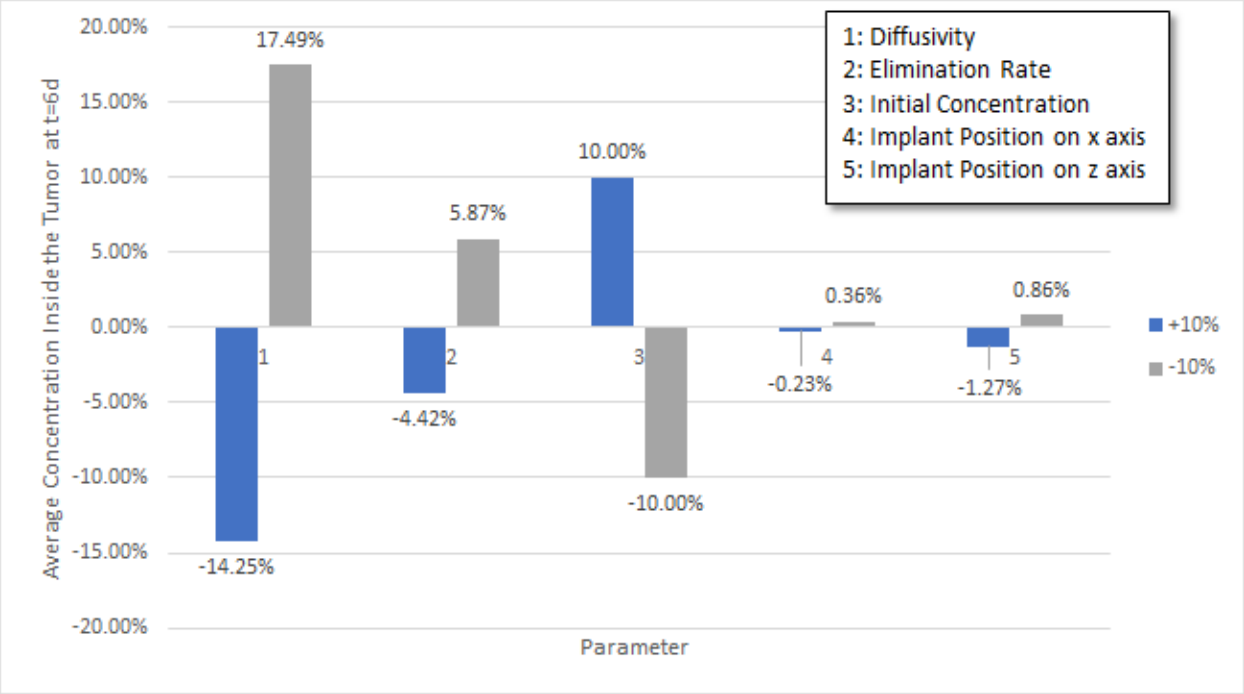

Figure 12: **Sensitivity analysis** performed by varying parameters by +/- 10 percent to analyze the average drug concentration inside the tumor at day 6.

As shown in Figure 12, we varied each parameter by increasing or decreasing their original value by 10% and then calculating the resulting percentage change in the average drug concentration. From the results, variation in either drug diffusivity and initial drug concentration would cause significant concentration changes in our model. Each parameter and its effect is examined thoroughly in the following graph.

Changing the implant position along x axis or z axis all resulted in mild changes in the drug concentration after 6 days. This lines up with projected expectations that the implant locations are not a major effect on the drug concentration change in the long run. As more drugs diffuse out of the implant with time, the average concentration difference caused by the implant location is neglectable.

Increasing the drug diffusivity results in lower concentration in the tumor, because more drugs can be diffused out in the same amount of time. Diffusivity describes how easily a substance can diffuse in the other substance. Higher diffusivity means easier diffusion process and more substances are diffused at the same time. Thus, higher drug diffusivity translates to a lower concentration inside the tumor.

Increasing the drug elimination rate reduced the drug concentration at day 6. As drug elimination rate is how fast drugs are consumed by the tumor, higher elimination rate means quicker consumption and causes lower drug concentration.

Increasing 10% initial drug concentration results in exactly 10% increase of the drug concentration. The linear dependence between initial drug concentration and average drug concentration inside at a given time need further computation and exploration.

Discussion

Layout of the Implants

From our concentration profile and average concentration over time plots above (Fig. 6, Fig. 7 and Fig 10), we can see that having multiple implants inside the tumor helped maintaining the concentration in the tumor larger than all the other options before the drug elimination starts at t=4d, which means better drug delivery.

We believe this advantage is due to the increase of surfaces through which the drug can diffuse out. Before the result, we had suspected that laying the implants closer to the boundary could increase concentration gradient, hence accelerating the drug to diffuse out of the tumor. But the result showed us that this can be offset by the extra drug coming out of the implants.

Shape of the implants

From our result (Fig. 6, Fig. 8, Fig. 9 and Fig. 10), we can observe that there are small but notifiable differences in the average concentrations of the three different shapes. At the same time, the spherical implant has the significantly lower average concentration value, while the rectangular and cylindrical ones are essentially the same.

We believe that this difference is caused by edge effects: the nodes on the edges are closer to the boundary, hence, the concentration gradient is higher at these nodes, which made the diffusion faster. Therefore, the more edges an implant has, the higher the average concentration it will be.

Based on these findings, and since we want to retain the drug inside the tumor relatively longer, we believe that the spherical implant is a worse choice.

Conclusion and future directions

From our computation, the best implant method is having multiple implants inside the tumor, and that as long as we don't use spherical shape, the shape of the implant doesn't matter too much in the sense of drug delivery.

We have several directions for future studies that can go from ours.

First, parameter optimization can be performed for the exact layout of the multiple implants: What is the optimum radius of the circle that circumscribes them? This is an applicable question because if we place the implants too close to the tumor boundary, the drug would diffuse out of the tumor too quickly; and if we place the implants too clustered at the center, we cannot fully make use of the extra surfaces that multiple implants provide.

Second, as we mentioned in the Validation part, one of the main sources of the error of our model comes from the inaccurate elimination rate. Therefore, in the future, more comprehensive experiments need to be carried out for us to more accurately model the change of elimination rate as a function of time ($\gamma = f(t)$).

At last, in medical reality, another drug, dexamethasone, is often added to prevent inflammation and fibrosis [6]. Therefore, adding dexamethasone as a new component into the model to understand its interaction with the drug release of doxorubicin is of practical significance.

Reference

[1] Geller DA, Tsung A, Marsh JW, Dvorchik I, Gamblin TC, Carr BI. 2006. Outcome of 1000 liver cancer patients evaluated at the UPMC Liver Cancer Center. J Gastrointest Surg 10:63–68.

[2] Blanco, Elvin, et al. "Local release of dexamethasone from polymer millirods effectively prevents fibrosis after radiofrequency ablation." Journal of Biomedical Materials Research Part A: An Official Journal of The Society for Biomaterials, The Japanese Society for Biomaterials, and The Australian Society for Biomaterials and the Korean Society for Biomaterials 76.1 (2006): 174-182.

[3] Gasselhuber, Astrid, et al. "Targeted drug delivery by high intensity focused ultrasound mediated hyperthermia combined with temperature-sensitive liposomes: computational modelling and preliminary in vivo validation." *International Journal of Hyperthermia* 28.4 (2012): 337-348.

[4] Francica G, Marone G. 1999. Ultrasound-guided percutaneous treatment of hepatocellular carcinoma by radiofrequency hyperthermia with a ‘cooled-tip needle’. A preliminary clinical experience. Eur J Ultrasound 9:145–153.

[5] Kochanek Kenneth D., M.A., Murphy Sherry, et al. Deaths: Final data for 2017. National vital statistics reports; vol 68 no 9. Hyattsville, MD: National Center for Health Statistics. 2019.

[6] Bentrem, David J., Ronald P. DeMatteo, and Leslie H. Blumgart. "Surgical therapy for metastatic disease to the liver." Annu. Rev. Med. 56 (2005): 139-156.

[7] Weinberg, Brent D., et al. "Polymer implants for intratumoral drug delivery and cancer therapy." Journal of pharmaceutical sciences 97.5 (2008): 1681-1702.

[8] Weinberg, Brent D., et al. "Modeling doxorubicin transport to improve intratumoral drug delivery to RF ablated tumors." Journal of controlled release 124.1-2 (2007): 11-19.

[9] Merkle EM, Boll DT, Boaz T, Duerk JL, Chung YC,Jacobs GH, Varnes ME, Lewin JS. 1999. MRI-guided radiofrequency thermal ablation of implanted VX2 liver tumors in a rabbit model:

Demonstration of feasibility at 0. 2 T. Magn Reson Med 42:141–149.

[10] Goldberg EP, Hadba AR, Almond BA, Marotta JS. 2002. Intratumoral cancer chemotherapy and immunotherapy: Opportunities for nonsystemic preoperative drug delivery. J Pharm Pharmacol 54:159–180.

[11] Curley SA, Izzo F, Delrio P, Ellis LM, Granchi J, Vallone P, Fiore F, Pignata S, Daniele B, Cremona F. 1999. Radiofrequency ablation of unresectable primary and metastatic hepatic malignancies: Results in 123 patients. Ann Surg 230:1–8.

[12] Varshney S, Sewkani A, Sharma S, Kapoor S, Naik S, Sharma A, Patel K. 2006. Radiofrequency ablation of unresectable pancreatic carcinoma: Feasibility, efficacy and safety. JOP 7:74–78.

[13] Nguyen CL, Scott WJ, Goldberg M. 2006. Radio-frequency ablation of lung malignancies. Ann Thorac Surg 82:365–371.
[14] Goldberg EP, Hadba AR, Almond BA, Marotta JS. 2002. Intratumoral cancer chemotherapy and immunotherapy: Opportunities for nonsystemic preoperative drug delivery. J Pharm Pharmacol 54:159–180.
[15] sun2003 pro follow. "Tumor-Small - 3D Model by sun2003 (@sun2003) [b19f2c2]." Sketchfab, 1 Sept. 1969, sketchfab.com/3d-models/tumor-small-b19f2c2fac4b4cf5b2299b611673cec6.

Appendices

Appendix A: COMSOL model variables

Table A1: Variables and parameter values used in the COMSOL model

Symbol	Value	Description	Reference
D	$8.76 * 10^{-11} m^2\ s^{-1}$	Diffusivity of doxorubicin inside the tumor	Weinberg et al.
γ	$0.00\ s^{-1}\ (t < 4\ days)$ $0.57 * 10^{-4}\ s^{-1}\ (t > 4\ days)$	Elimination rate	Weinberg et al.
q''	Varies in the model	Drug flux	Weinberg et al.
$R_{single-cylindrical-implant}$	$0.75\ mm$	Single cylindrical implant radius	Weinberg et al.
$Height_{single-cylindrical-im}$	$8\ mm$	Single cylindrical implant height	Weinberg et al.
$R_{four-cylindrical-implant}$	$0.55\ mm$	Four cylindrical implant radius	
$Height_{four-cylindrical-imp}$	$4\ mm$	Four cylindrical	

		implant height	
$r_{four-cylindrical-implant}$	$1.8\,mm$	Four cylindrical implant distance towards center	
$R_{single-spherical-implant}$	$1.5\,mm$	Single spherical implant radius	
$Width_{single-block-implant}$	$1.33\,mm$	Single block implant width	
$Depth_{single-block-implant}$	$1.33\,mm$	Single block implant depth	
$Height_{single-block-implant}$	$8\,mm$	Single block implant height	

Appendix B: Memory and time

Figure B1: The CPU time taken and the memory being used by a typical run.

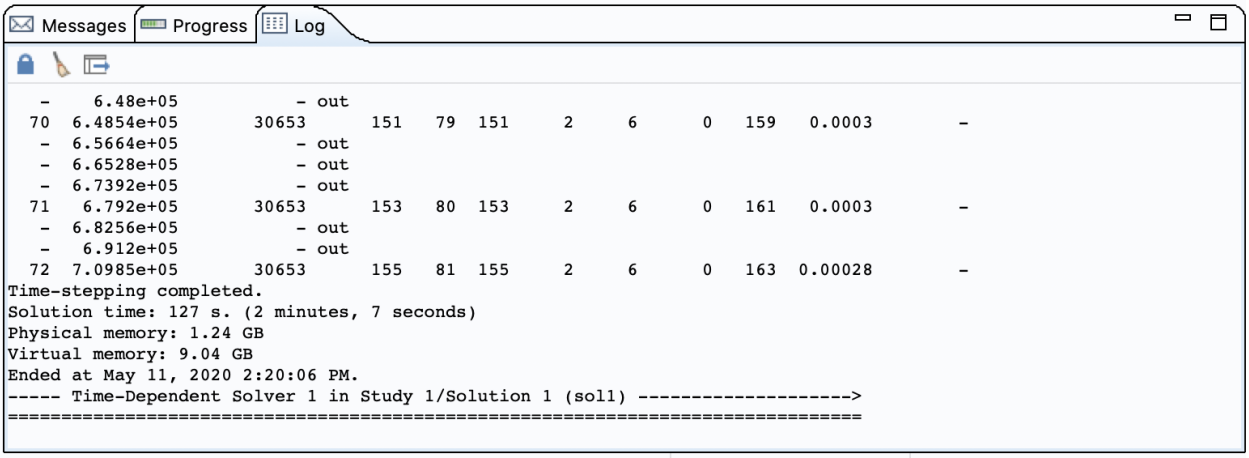

Supplement Material

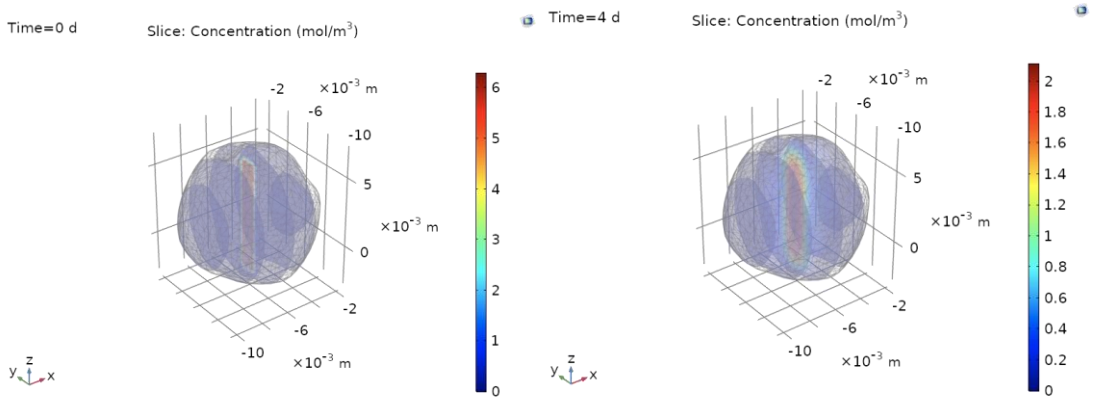

Figure S1: **Concentration profile inside the tumor with a single implant between 0, 4 days**. At the initial state (t=0 days), there is no drug in the tumor domain and all the drug is inside the implant. When t = 4 days, ~68% drug diffuses out from the implant into the tumor as seen by the increased 'redness' from the model which correlates to increased drug concentration.

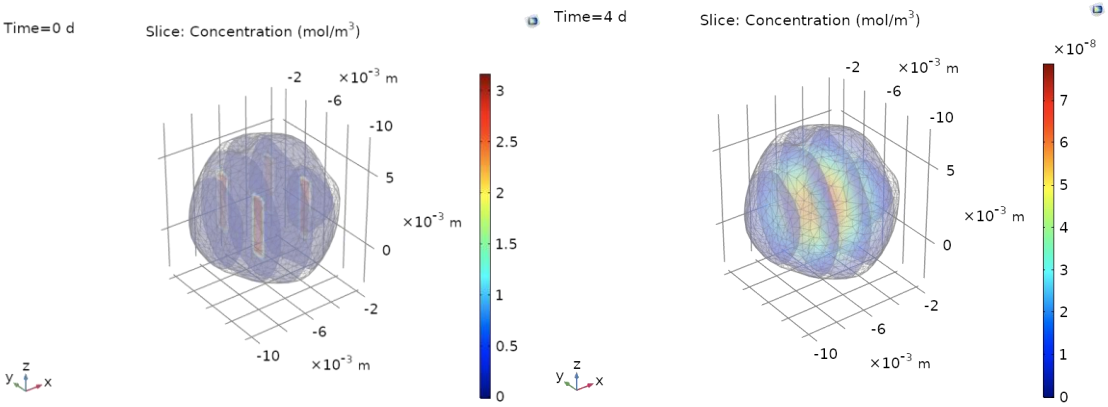

Figure S2: **Concentration profile inside the tumor with 4 implants between 0, 4 days**. At the initial state (t=0 days), there is no drug in the tumor domain and all the drug is inside the implant. When t = 4 days, plenty of drug diffuses out from the implant into the tumor as seen by the increased 'redness' from the model which correlates to increased drug concentration.

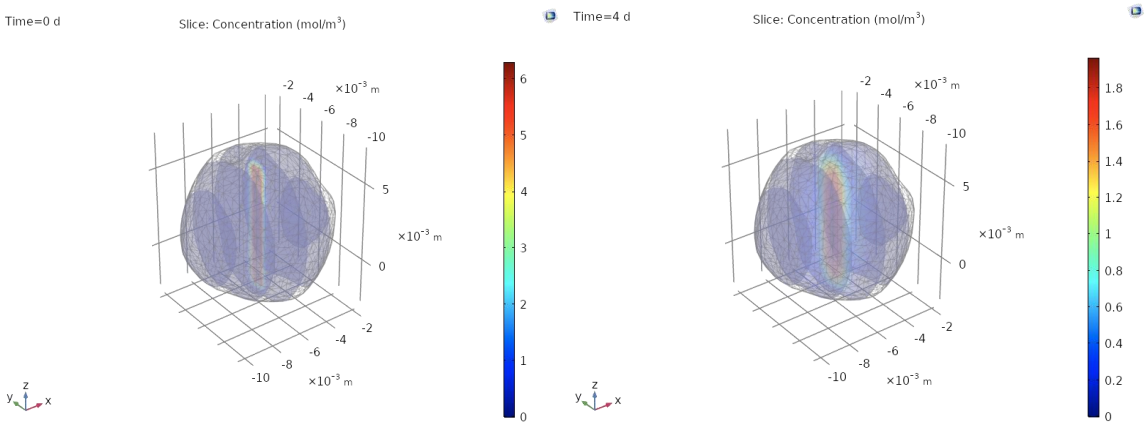

Figure S3: **Concentration profile inside the tumor with rectangular prism implants between 0, 4 days**.

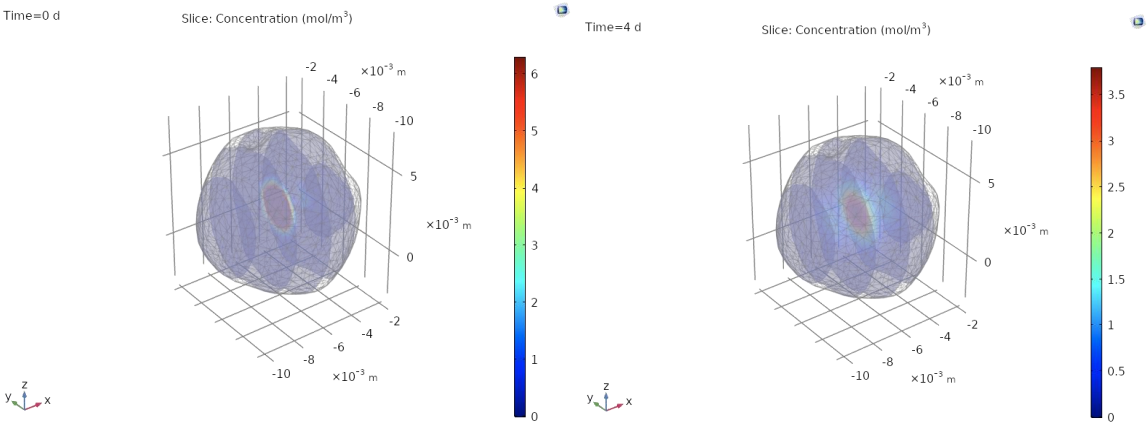

Figure S4: **Concentration profile inside the tumor with spherical implants between 0, 4, and 8 days**.